UCLA
UCLA Previously Published Works

Title
Three-dimensional posture changes of the vocal fold from paired intrinsic laryngeal muscles

Authors
Vahabzadeh-Hagh, Andrew M
Zhang, Zhaoyan
Chhetri, Dinesh K

Peer reviewed

Three Dimensional Posture Changes of the Vocal Fold from Paired Intrinsic Laryngeal Muscles

Andrew M. Vahabzadeh-Hagh, MD[a], **Zhaoyan Zhang, PhD**[a], and **Dinesh K. Chhetri, MD**[a]

[a]Department of Head and Neck Surgery, UCLA David Geffen School of Medicine, 10833 Le Conte Ave, 62-132, Los Angeles, CA USA 90095

Abstract

Objective—Although the geometry of the vocal fold medial surface affects voice quality and is critical in the treatment of glottic insufficiency, the pre-phonatory shape of the vocal fold medial surface is not well understood. In this study, we activated intrinsic laryngeal muscles (ILMs) individually and in combinations, and recorded the temporal sequence and precise three-dimensional configurational changes of the vocal fold medial surface.

Study Design—*In vivo* canine hemilarynx model.

Methods—A hemilaryngectomy was performed in an *in vivo* canine and ink was used to mark the medial surface of the *in situ* vocal fold in a grid-like fashion. The thyroarytenoid (TA), lateral cricoarytenoid (LCA), cricothyroid (CT), and posterior cricoarytenoid (PCA) muscles were stimulated individually and in combinations. A right angle prism whose hypotenuse formed the glottal midline provided two distinct views of the medial surface for a high-speed digital camera. Image-processing package DaVis (LaVision Inc.) allowed time series cross-correlation analysis for 3-dimensional deformation calculations of the vocal fold medial surface.

Results—Combined TA and LCA activation yields an evenly adducted rectangular glottal surface. Addition of thyroarytenoid to cricoarytenoid adducts the vocal fold from inferior to superior in a graded fashion allowing formation of a divergent glottis. Posterior cricoarytenoid has a bimodal relationship with thyroarytenoid favoring abduction. Cricothyroid and lateral cricoarytenoid yield unique glottal postures necessary but likely not sufficient for phonation.

Conclusions—Understanding the three-dimensional geometry of the vocal fold medial surface will help us better understand the cause-effect relationship between laryngeal physiology and phonation.

CORRESPONDING AUTHOR: Andrew M. Vahabzadeh-Hagh, AVahabzadehHagh@mednet.ucla.edu, Phone: 310-825-4949, Fax: 310-206-1393, Address: 10833 Le Conte Ave, 62-132, Los Angeles, CA USA 90095.

Keywords

INTRODUCTION

Phonation results from the interaction between aerodynamic forces acting upon the vocal fold pre-phonatory posture. Neuromuscular activation of the intrinsic laryngeal muscles (ILMs) provides precise control of the vocal fold pre-phonatory posture, which includes glottal tension, stiffness, and medial surface shape. The vocal fold posture has strong influence on the fluid-structure interactions and resulting vocal fold vibratory mode, phonation type, and the conversion of aerodynamic power to acoustic power. Better understanding muscular control of vocal fold geometry is thus a critical aspect of better understanding the mechanisms of voice production and how geometric modifications of vocal fold contour, such as with injection or type I thyroplasty, will impact fundamental parameters of voice.

Glottal channel shape or geometry is primarily orchestrated by four pairs of ILMs: the thyroarytenoid (TA), lateral cricoarytenoid (LCA), cricothyroid (CT), and posterior cricoarytenoid (PCA) muscles [1,2]. Optimizing the medial surface shape has been shown to lower phonation threshold pressures and improve vocal efficiency [3-7]. Glottal channel shape, as achieved through differential activation of the ILMs determines voice quality and permits vocal register and pitch control [8-10]. Herbst et al demonstrated 4 unique voice qualities resulting from 4 distinct glottal configurations as assessed by videostroboscopy, videokymography, and electroglottography [11]. Kochis-Jennings et al used electromyography to show TA dominant phonation at lower fundamental frequencies, below 200-300 Hz, and CT dominant phonation for chest, head, and falsetto phonation above 200-300 Hz [12,13]. Doellinger showed that TA activation alone achieves chest-like vibrations at low activation levels and fry-like vibrations with higher activation [14,15].

Understanding how phonatory posture controls voice production, and what posture parameters could be manipulated with voice therapy or surgery has been limited by lack of quantitative measurements of glottal channel shape with ILM activation. Specifically, the medial surface of the vocal folds undergoes 3-dimensional posture changes that simply cannot be assessed from the standard 2-dimensional endoscopic view. To better understand the interaction between vocal fold medial surface geometry and the resulting voice, a direct and systematic investigation of muscular control of vocal fold geometry is needed. In this report, we use the most direct means of observing the vocal fold medial surface, a sagittal hemilarynx view, in a neuromuscularly intact *in vivo* canine model. We provide precise stimulation of individual ILMs from baseline to full activation in a graded fashion, and evaluate the interaction of pairs of ILMs in controlling pre-phonatory posture.

MATERIALS AND METHODS

This study was approved by the Institutional Animal Care and Use Committee. Three mongrel canines were used with similar findings but for consistency, data is presented from

one canine. With the canine under general anesthesia a transcervical right hemilaryngectomy was performed as previously described [1,2]. Fleshpoints were marked in a grid-like fashion on the medial surface of the left vocal fold using India ink. The glottic midline of the intact left hemilarynx was directly opposed to the hypotenuse of a right-angle glass prism. The prism provides two distinct views of the left vocal fold medial surface captured by a high-speed digital camera. These two distinct views allowed for stereo measurements and 3-dimensional space reconstruction using the image-processing program DaVis (LaVision Inc., Goettingen, Germany). Here we used a right-angle prism to allow visualization of the entire vocal fold medial surface throughout the spectrum of its posture changes as demonstrated feasible in prior reports [14,16-19]. A high-speed digital camera (Phantom v210, Vision Research Inc., Wayne, NJ) captured medial surface motion at 3,000 frames per second. The camera (384 x 672 pixel resolution; 0.04 mm/pixel) was calibrated to a standardized calibration plate [20]. DaVis utilizes the fleshpoints and finer random surface pixel variation for image correlation and surface height calculation. *Surface height*, defined as the distance from the vocal fold medial surface to the prism or glottic midline was calculated. MATLAB was used to process surface height data sets to create 3D contour plots of the medial surface.

For neuromuscular stimulation of ILMs, branches of the recurrent laryngeal nerve (RLN) to the PCA and TA were isolated, ligated, and each fashioned with a cuff electrode. The RLN main trunk was used to stimulate LCA/IA muscle complex. The external branch of the superior laryngeal nerve (SLN) was isolated and used to stimulate the CT muscle. Neuromuscular stimulation was performed as previously described, 0.1 ms cathodic pulses at 100Hz for 1,500 ms [2]. Graded activation of the individual ILMs was performed over 7 equally spaced levels; from level 1, threshold muscle activation, to level 7, supramaximal activation. For data analysis, the stimulation grade beyond which no further change in final glottal posture was observed was selected as the maximum stimulation grade for each muscle; namely, grade 5 for TA and 6 for the others (LCA, CT, PCA). We then evaluated the interactions between the following 8 pairs of muscle activation conditions: (1) TA (maximal activation, "max") – LCA (graded activation from zero to maximal activation, "graded"), (2) LCA (max) – TA (graded), (3) TA (max) – CT (graded), (4) CT (max) – TA (graded), (5) TA (max) – PCA (graded), (6) PCA (max) – TA (graded), (7) CT (max) – LCA (graded), (8) LCA (max) – CT (graded).

RESULTS

Thyroarytenoid and Lateral Cricoarytenoid Muscle Interactions

Figure 1 shows glottal shape changes over time in a color-coded format detailing the 3D deformation for interactions between TA maximal activation/LCA graded activation. Columns correspond to temporal sequence of medial surface shape changes following stimulation. Far left column is time zero (resting posture) and each subsequent rightward column is some time interval later. Total duration displayed is 50 ms capturing complete posture change. Each row then corresponds to a different LCA activation level specified by the row title. The first row is maximal TA activation with no LCA activation ('LCA 0', LCA grade 0). Subsequent rows demonstrate posture changes for increasing LCA activation in combination with full TA activation. Posterior glottal closure is seen for LCA grades 3-6.

The TA provides near complete closure of the mid membranous vocal fold, 96% adduction relative to resting glottal width calculated for a point midway between the anterior commissure and the vocal process along the glottal axis and midway between the superior and inferior edge of the vocal fold along the vertical axis. Full TA yields a 5% shortening of the vocal fold in the anteroposterior dimension and an 8% thickening of the mid-to-anterior vocal fold in vertical height. With increasing LCA stimulation the thickening of the vocal fold involves the more mid-to-posterior part of the vocal fold creating a more homogeneously thickened and adducted rectangular posture.

Figure 2 shows glottal shape changes with full LCA activation (grade 6) with graded TA activation. First row corresponds to LCA grade 6, TA grade 0, and subsequent rows represent increasing TA from grade 0 to 5. Increased adduction is apparent beginning with TA grade 3. TA increases adduction of the mid-point of the vocal fold, calculated as described earlier, from 82% with LCA, to 95% with full TA. Lastly, added TA shifts vertical height thickening from the posterior to the mid-to-anterior vocal fold.

Thyroarytenoid and Cricothyroid Muscle Interactions

Figure 3 shows glottal shape changes for maximal TA activation and graded CT activation. Duration was 117 ms capturing complete posture change with the slower CT muscle. TA shortens the vocal fold by 11% while CT activation lengthens the vocal fold back to its resting length. By 117 ms TA activation thickens the anterior vocal fold by 18%, an effect that is reversed to a net 20% thinning with maximum CT.

Figure 4 shows glottal shape changes for maximal CT activation with graded TA activation. CT activation alone (row 1) yields 25% abduction of the mid vocal fold. CT alone lengthens the vocal fold by 8% which is countered by TA. CT also thins the vertical height of the vocal fold throughout (posterior, mid, and anterior cord). With combined activation of full CT and TA grades 1-3 the vocal fold is lengthened, thinned, and the inferior mid-to-anterior cord fully adducted (divergent glottis). The superior aspect of the vocal fold medial surface under these conditions, partially adducted, may contribute to phonation differently than when more taught and fully adducted for greater TA activation.

Thyroarytenoid and Posterior Cricoarytenoid Muscle Interactions

Figure 5 shows the glottal shape changes over time for TA maximal activation (first row), with graded PCA activation for subsequent rows (grade 1 to 6). TA adduction is countered by PCA grade 6, bringing the vocal fold nearly back to its baseline glottal width. TA shortens the vocal fold which is subsequently lengthened with PCA activation. Increasing PCA activation leads to more evenly distributed vertical thickness in the anteroposterior glottal axis.

Figure 6 shows results for maximal PCA activation (grade 6, all rows) with graded TA activation. PCA provides robust 75% abduction of the mid vocal fold which is reversed for mid-level TA activation (grades 2-3) but not for higher TA grades, suggesting that when PCA and TA activation levels are comparable, PCA takes priority. PCA results in 5%

lengthening, which is then reversed with TA activation. PCA also slightly thickens the vocal fold, an effect which is augmented with TA activation.

Lateral Cricoarytenoid and Cricothyroid Muscle Interactions

Figure 7 shows glottal shape changes for max CT activation (grade 6, all rows), with graded LCA activation. Duration is 67 ms capturing complete posture change. CT alone provides mild abduction (16%) that is countered with LCA activation to an overall mid cord adduction of 63% with LCA grade 6. CT lengthens the vocal fold by 12% regardless of LCA grade. CT also thins the vocal fold's vertical height. With increasing LCA activation the vertical height is further thinned to achieve an 18% reduction. Adduction caused by LCA when the CT already has tone, is homogeneous, spread along the entire medial surface, as opposed to being centered on the posterosuperior edge.

Figure 8 shows glottal shape changes for maximal LCA activation with graded CT activation. LCA alone adducts the mid cord by 88%. The addition of CT causes some abduction, resulting in a net adduction of 64%. CT increases the vocal fold length. LCA alone thins the vocal fold's vertical height. The addition of CT activation further thins vertical height by 19%. The vocal fold acts more like a single rigid structure when CT is active, allowing the LCA effect to be more evenly distributed along the length of the vocal fold.

DISCUSSION

An appreciation for the importance of glottal configuration in phonation dates back at least to the mid twentieth century and has driven us to find ways to observe the glottal channel during vocal fold vibration [17,21-24]. Unfortunately, most efforts have resulted in indirect observation providing conjectures as opposed to answers. Fink and Kirschner visualized the phonating human vocal folds using x-ray tomography in 1959. They observed a convex infraglottic shape, an exponential curve, believed to yield the lowest coefficient of flow resistance, optimizing phonatory efficiency [22]. In the 1970s, Hirano looked at excised canine larynges frozen after muscular stimulation and also found this medial TA bulge [25]. Here we provide the most direct and neuromuscularly intact view of the vocal fold medial surface under various prephonatory conditions. In so doing, we hope to help validate prior laryngeal modeling research and better relate anatomic changes to the concept of different phonatory modes.

TA works to shorten, thicken, and adduct the vocal fold. Figure 1 shows the effect of combining graded LCA activation to TA, which provides more complete posterior adduction and evens out the vertical thickening of the vocal fold along the glottal axis. This yields a more homogenous, rectangular glottal channel.

CT activation alone yields vocal fold lengthening, vertical height narrowing, and mild abduction (Figure 4). With the CT fully engaged, increasing TA activation yields first adduction of the inferior aspect of the vocal fold (TA grades 1-3) creating a divergent glottis. This perhaps provides enough adduction to reduce phonation threshold pressure while maintaining the lengthening effect of CT to keep tension on the superior cord achieving a

particular phonatory mode. Increasing TA activation yields more complete adduction and shortening of the vocal fold. Perhaps it is in this mode, where the effects of CT have been near neutralized, that the relationship between TA activation and F0 are reversed as Doellinger described [14]. The TA is one of the major contributors to the elastic modulus of the vocal folds and the CT is often synergistic. However, there is some evidence that high TA activation levels may be antagonistic to CT reducing the elastic modulus of the vocal folds [10,15]. Here we see the anatomic correlate with high TA and full CT activation (Figure 4).

PCA activation causes vocal fold lengthening, vertical thickening, and abduction (Figure 6). Figures 5 and 6 depict the tug of war between the TA and PCA in regards to vocal fold length and adduction. In Figure 5 high grade PCA activation is able to overcome TA adduction. Figure 6 depicts a unique bimodal relationship to increasing TA activation. For mid-grade (2-3), TA causes mid-to-anterior vocal fold adduction, however with higher grades (4-5) the adductory effects of TA are lost. This bimodal relationship suggests perhaps a default gating of laryngeal innervation which favors vocal fold abduction over adduction during maximal laryngeal stimulation; perhaps evidence of a laryngeal abductor reflex, a proprioceptive laryngeal feedback loop or related to size and/or fiber-type composition of the TA versus PCA. Nevertheless, the multifaceted larynx, designed to protect and maintain the airway, favors airway patency under maximal neuromuscular input.

Lastly we see the interplay between the CT and LCA muscles in Figures 7 and 8. Here LCA and CT activated in isolation or various combinations yields vertical height narrowing. When CT is incrementally added to LCA, the abductory effect of CT is more apparent than with TA. Interestingly when LCA is added to CT, the adduction imparted by LCA is homogenous in the glottal axis as opposed to its more posterosuperior focal point when activated alone. Full CT activation may provide enough vocal fold stiffness that the adductory forces of the LCA are evenly distributed along its length. Although unique medial surface geometries are achieved with combinations of LCA and CT, the vocal fold only achieves 16 to 83% adduction, highlighting their role as a phonatory modulator as opposed to driver.

Optimizing vocal efficiency is the goal whether for sport in the vocal athlete or for easing everyday life in those stricken with glottic insufficiency. The question remains as to what glottal geometry is optimal in these conditions. Titze showed that a divergent glottis provides lower oscillation threshold pressures and greater ease of phonation. Other modeling studies have favored a rectangular or slightly convergent glottis [6,26-28]. Regardless, this study shows the intricate control and vast geometric possibilities capable with individual and combined ILM activations. A rectangular configuration is achieved with full TA and LCA activation, a divergent glottis with full CT and mid TA activation, and a convergent glottis with full CT and mid-to-full LCA activation. As such, muscular control of the TA, LCA, and CT are critical determinants of the great variety of possible glottal postures [29].

This report is the beginning in our efforts to understand how glottal form allows versatility in human phonation. As Titze described the 4 quadrants of phonation (speech, falsetto, chest, and pressed phonation), the low and intermediate activation levels of the combined ILMs

remains to be evaluated [30]. Here we relate glottal postures to acoustic measures as found in the literature. In future work, we will evaluate the dynamic changes of the vocal fold geometry during phonation and directly measure resulting acoustics. Ultimately this will provide us with the most direct assessment of glottal form to function.

CONCLUSION

Combined activation of the intrinsic laryngeal muscles allows an amazing and vast variety of unique prephonatory glottal postures, creating a strikingly adaptable instrument to a wide array of phonatory types. Combinations of TA, LCA, and CT can form a rectangular, divergent, or convergent glottis, providing the necessary glottal posture for maximum vocal efficiency. TA and CT dominant postures may correspond to different phonatory modes. Combined PCA and TA provides a unique bimodal relationship that favors vocal fold abduction. Lastly, CT and LCA yield unique glottal postures likely necessary but not sufficient for normal phonation. Prephonatory posture is the critical substrate for voice production. Understanding prephonatory posture may improve our understanding of normal and abnormal voice production, better guiding our therapeutic efforts.

ACKNOWLEDGMENTS

REFERENCES

1. Chhetri DK, Neubauer J, Bergeron JL, Sofer E, Peng KA, Jamal N. Effects of asymmetric superior laryngeal nerve stimulation on glottic posture, acoustics, vibration. The Laryngoscope. 2013; 123(12):3110–3116. [PubMed: 23712542]

2. Chhetri DK, Neubauer J, Berry DA. Graded activation of the intrinsic laryngeal muscles for vocal fold posturing. J Acoust Soc Am. 2010; 127(4):El127–133. [PubMed: 20369979]

3. Mau T, Muhlestein J, Callahan S, Chan RW. Modulating phonation through alteration of vocal fold medial surface contour. The Laryngoscope. 2012; 122(9):2005–2014. [PubMed: 22865592]

4. Scherer RC, Shinwari D, De Witt KJ, Zhang C, Kucinschi BR, Afjeh AA. Intraglottal pressure profiles for a symmetric and oblique glottis with a divergence angle of 10 degrees. J Acoust Soc Am. 2001; 109(4):1616–1630. [PubMed: 11325132]

5. Scherer RC, Shinwari D, De Witt KJ, Zhang C, Kucinschi BR, Afjeh AA. Intraglottal pressure distributions for a symmetric and oblique glottis with a uniform duct. J Acoust Soc Am. 2002; 112(4):1253–1256. [PubMed: 12398430]

6. Titze IR. The physics of small-amplitude oscillation of the vocal folds. J Acoust Soc Am. 1988; 83(4):1536–1552. [PubMed: 3372869]

7. Courey MS. Homologous collagen substances for vocal fold augmentation. The Laryngoscope. 2001; 111(5):747–758. [PubMed: 11359151]

8. Titze IR. A framework for the study of vocal registers. Journal of voice : official journal of the Voice Foundation. 1988; 23:1–12.

9. Vilkman E, Alku P, Laukkanen AM. Vocal-fold collision mass as a differentiator between registers in the low-pitch range. Journal of voice : official journal of the Voice Foundation. 1995; 9(1):66–73. [PubMed: 7757152]

10. Zhang Z. Cause-effect relationship between vocal fold physiology and voice production in a three-dimensional phonation model. J Acoust Soc Am. 2016 In Press.

11. Herbst CT, Ternstrom S, Svec JG. Investigation of four distinct glottal configurations in classical singing--a pilot study. J Acoust Soc Am. 2009; 125(3):El104–109. [PubMed: 19275279]

12. Kochis-Jennings KA, Finnegan EM, Hoffman HT, Jaiswal S. Laryngeal muscle activity and vocal fold adduction during chest, chestmix, headmix, and head registers in females. Journal of voice : official journal of the Voice Foundation. 2012; 26(2):182–193. [PubMed: 21596521]

13. Kochis-Jennings KA, Finnegan EM, Hoffman HT, Jaiswal S, Hull D. Cricothyroid muscle and thyroarytenoid muscle dominance in vocal register control: preliminary results. Journal of voice : official journal of the Voice Foundation. 2014; 28(5):652.e621–652.e629.

14. Dollinger M, Berry DA, Berke GS. Medial surface dynamics of an in vivo canine vocal fold during phonation. J Acoust Soc Am. 2005; 117(5):3174–3183. [PubMed: 15957785]

15. Berke GS, Gerratt BR. Laryngeal biomechanics: an overview of mucosal wave mechanics. Journal of voice : official journal of the Voice Foundation. 1993; 7(2):123–128. [PubMed: 8353625]

16. Abdel-Aziz Y, Karara H. Direct linear transformation from comparator coordinates into object space coordinates in close-range photogrammetry. ASP Symp on Close Range Photogrammetry. 1971

17. Berry DA, Montequin DW, Tayama N. High-speed digital imaging of the medial surface of the vocal folds. J Acoust Soc Am. 2001; 110(5):2539–2547. Pt 1. [PubMed: 11757943]

18. Chen L, Armstrong CW, Raftopoulos DD. An investigation on the accuracy of three-dimensional space reconstruction using the direct linear transformation technique. Journal of biomechanics. 1994; 27(4):493–500. [PubMed: 8188729]

19. Doellinger M, Berry DA, Berke GS. A quantitative study of the medial surface dynamics of an in vivo canine vocal fold during phonation. The Laryngoscope. 2005; 115(9):1646–1654. [PubMed: 16148711]

20. Zhang Z, Neubauer J, Berry DA. Aerodynamically and acoustically driven modes of vibration in a physical model of the vocal folds. J Acoust Soc Am. 2006; 120(5):2841–2849. Pt 1. [PubMed: 17139742]

21. Farnsworth D. High-speed motion pictures of the human vocal cords. Bell Lab. 1940; Rec 18:203–208.

22. Fink BR, Kirschner F. Observations on the acoustical and mechanical properties of the vocal folds. Folia Phoniatr (Basel). 1959; 11:167–172. [PubMed: 13822887]

23. Hess MM, Ludwigs M. Strobophotoglottographic transillumination as a method for the analysis of vocal fold vibration patterns. Journal of voice : official journal of the Voice Foundation. 2000; 14(2):255–271. [PubMed: 10875578]

24. Saito, S., Fukuda, H., Isohai, Y., Ono, H. X-ray stroboscopy. In: Stevens, K., editor. Vocal Fold Physiology. University of Tokyo; Tokyo: 1981. p. 95-106.

25. Hirano M. Vocal Mechanisms in Singing: Laryngological and Phoniatric Aspects. Journal of Voice. 1988; 2(1):51–69.

26. Chan RW, Titze IR, Titze MR. Further studies of phonation threshold pressure in a physical model of the vocal fold mucosa. J Acoust Soc Am. 1997; 101(6):3722–3727. [PubMed: 9193059]

27. Lucero JC. Optimal glottal configuration for ease of phonation. Journal of voice : official journal of the Voice Foundation. 1998; 12(2):151–158. [PubMed: 9649070]

28. Zhang Z. Influence of flow separation location on phonation onset. J Acoust Soc Am. 2008; 124(3):1689–1694. [PubMed: 19045659]

29. Chhetri DK, Neubauer J. Differential roles for the thyroarytenoid and lateral cricoarytenoid muscles in phonation. The Laryngoscope. 2015; 125(12):2772–2777. [PubMed: 26198167]

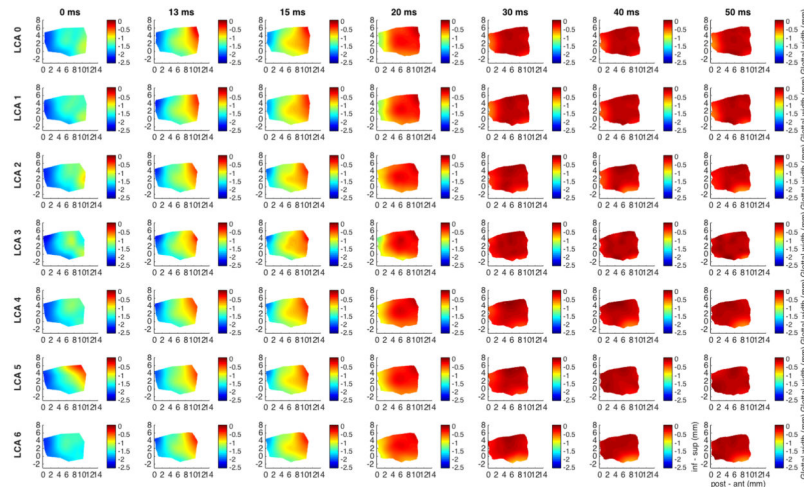30. Titze, IR. Principles of Voice Production. National Center for Voice and Speech; Iowa City, IA: 2000. p. 281-303.

Fig. 1.
Glottal shape for the interaction between maximal TA activation and graded LCA activation. Columns correspond to temporal sequence of medial surface shape changes following ILM stimulation starting at the left-most column, 0 ms, rest. Each subsequent column is then some time interval later as denoted by the title above each column. Total recorded duration was 50 ms. Each row corresponds to a particular ILM combination. All rows have full TA activation (grade 5) but LCA grade varies by row with grade 0, or no LCA, for row 1 and increasing LCA grades for subsequent rows as denoted by the title beside each row; 'LCA 0' corresponds to LCA activation grade 0. Each plot is a color-coded contour plot of the vocal fold medial surface. Left edges is posterior (vocal process), right edge is anterior (anterior commissure), inferior edge is inferior, superior edge is superior. Colorbar denotes surface height or glottal width; the distance from the vocal fold medial surface to the glottal midline; midline is denoted as '0'. Each subsequent figure is designed in this exact same format except a different muscle with be held at maximum stimulation while another muscle is added in a graded fashion. TA provides robust near complete adduction of the mid membranous vocal fold (96%, row 1). This level of adduction is maintained with combined graded LCA activation. Further, TA shortens the vocal fold by 5% and thickens it in the vertical dimension by 8%. Thickening is more evenly distributed in the glottal anteroposterior axis with LCA activation and adduction is overall more complete for the entire medial surface. Posterior glottal closure is seen for LCA grades 3-6 and is observed as early as 20 ms. Final posture is rectangular with full TA and LCA activation. (inf – sup = inferior to superior, LCA = lateral cricoarytenoid, ms = millisecond, post – ant = posterior to anterior, TA = thyroarytenoid).
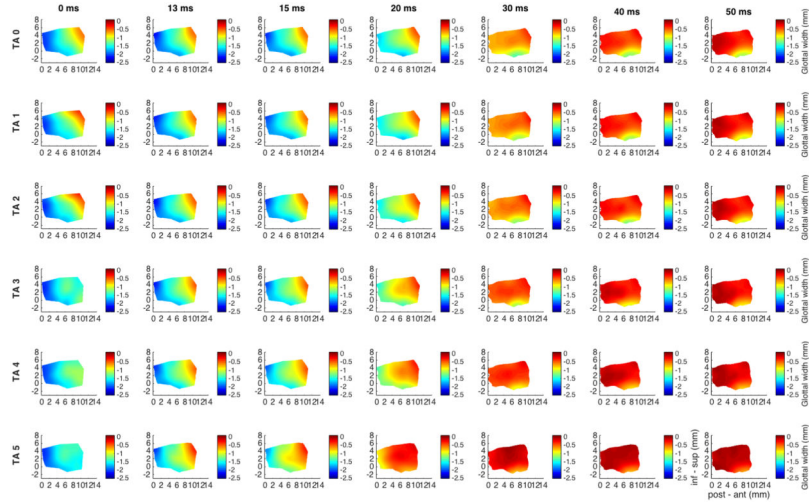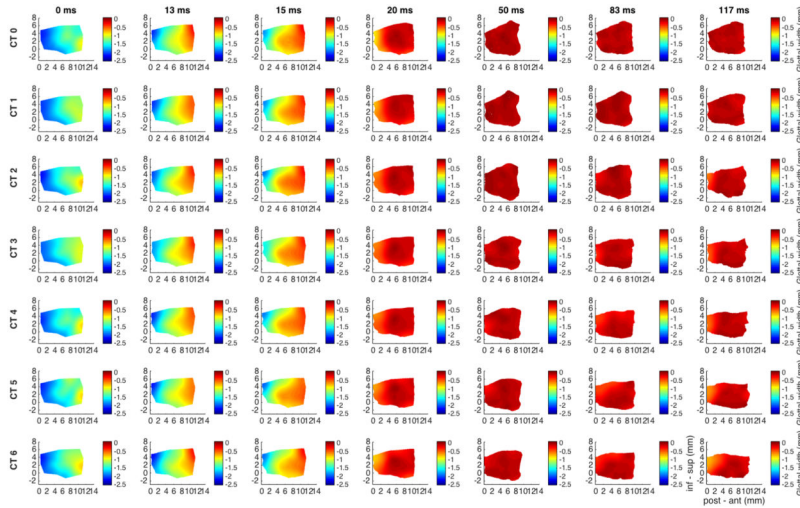
Fig. 2.
Glottal shape for the interaction between maximal LCA activation and graded TA activation. Design layout is same as Fig.1 except now LCA is held at maximum stimulation for all rows (grade 6), while TA is added in a graded fashion from grade 0 ('TA 0', row 1) to grade 5 ('TA 5', row 6). Increased adduction is apparent as early as 13 ms for TA stimulation grade 3 and above. TA increases overall mid-point adduction from 82% with LCA alone to 95% with full TA grade 5 activation. LCA alone (row 1) results in 3.5% vocal fold shortening and a 4-7% vertical height narrowing. Added TA shifts vertical height thickening to the mid-to-anterior vocal fold with increased grade of activation. (inf – sup = inferior to superior, LCA = lateral cricoarytenoid, ms = millisecond, post – ant = posterior to anterior, TA = thyroarytenoid).

Fig. 3.
Glottal shape for the interaction between maximal TA activation and graded CT activation. Design layout is same as Fig.1 except now TA is held at maximum stimulation for all rows (grade 5), while CT is added in a graded fashion from grade 0 ('CT 0', row 1) to grade 6 ('CT 6', row 7). CT is a slower acting ILM and as such duration of recording was extended to 117 ms to capture complete posture change. TA maintains a 95% vocal fold adduction irrespective of CT activation. The effects of CT appear to be evident beginning at grade 3 and a latency of 83 ms. TA shortens the vocal fold by 11% while CT activation neutralizes this effect. TA alone thickens the anterior vocal fold by 18%. With maximum CT added activation the anterior medial surface is net 20% thinner than baseline in the vertical dimension. (CT = cricothyroid, inf – sup = inferior to superior, ms = millisecond, post – ant = posterior to anterior, TA = thyroarytenoid).
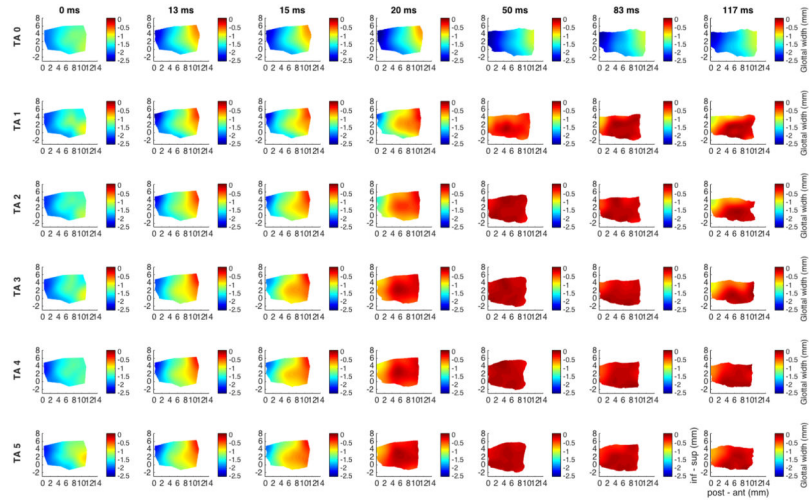
Fig. 4.
Glottal shape for the interaction between maximal CT activation and graded TA activation. Design layout is same as Fig.1 except now CT is held at maximum stimulation for all rows (grade 6), while TA is added in a graded fashion from grade 0 ('TA 0', row 1) to grade 5 ('TA 5', row 6). CT activation alone (row 1) results in 25% abduction, 8% lengthening, and 15% narrowing of the mid cord vertical height. TA activation provides dramatic 95-98% adduction beginning at grade 1. CT combined with TA grades 1-3 yields preferential adduction of the inferomedial vocal fold resulting in a divergent glottal configuration. Greater TA activation yields more uniform adduction of the full vertical thickness of the vocal fold. (CT = cricothyroid, inf – sup = inferior to superior, ms = millisecond, post – ant = posterior to anterior, TA = thyroarytenoid).
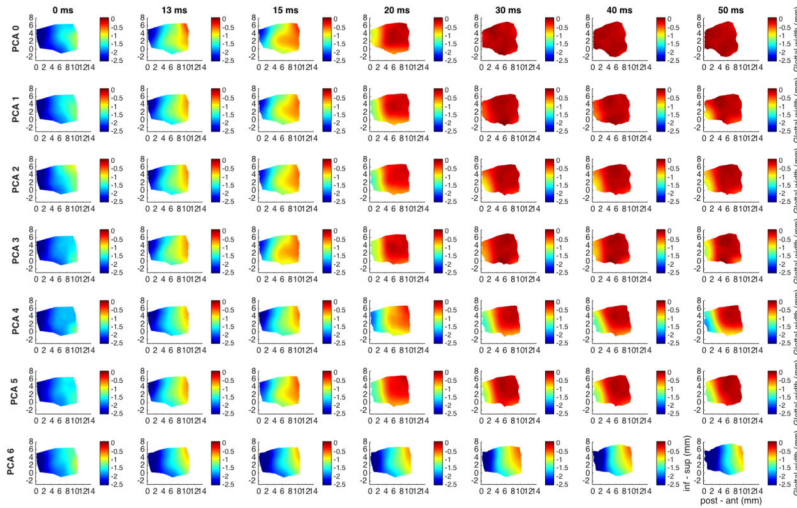
Fig. 5.
Glottal shape for the interaction between maximal TA activation and graded PCA activation. Design layout is same as Fig.1 except now TA is held at maximum stimulation for all rows (grade 5), while PCA is added in a graded fashion from grade 0 ('PCA 0', row 1) to grade 6 ('PCA 6', row 7). TA provides robust 95% adduction of the mid vocal fold, which is countered by PCA grade 6 abducting the mid-to-posterior cord back to its near baseline glottal width. The PCA also counteracts vocal fold shortening by the TA and improves the distribution of vertical height thickness in the anteroposterior glottal axis while mildly thinning the vocal fold relative to full independent TA activation. (inf – sup = inferior to superior, ms = millisecond, PCA = posterior cricoarytenoid, post – ant = posterior to anterior, TA = thyroarytenoid).
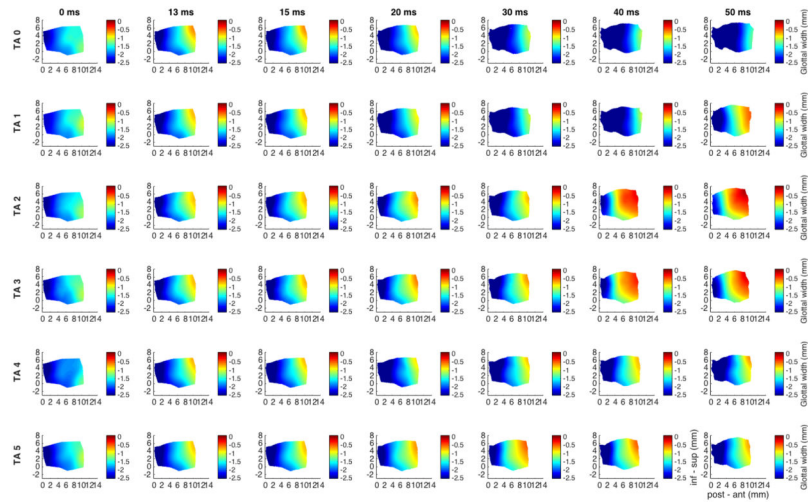
Fig. 6.
Glottal shape for the interaction between maximal PCA activation and graded TA activation. Design layout is same as Fig.1 except now PCA is held at maximum stimulation for all rows (grade 6), while TA is added in a graded fashion from grade 0 ('TA 0', row 1) to grade 5 ('TA 5', row 6). PCA abducts the mid vocal fold by 75%, lengthens it by 5% and maintains near baseline to subtle increase in vertical height thickness. Mid-level TA activation (grade 2-3) results in 45-60% adduction, near completely reversing the abductory effects of PCA. Higher-level TA activation (grade 4-5) fails to reverse the abductory effects of the PCA suggesting a priority for vocal fold abduction or airway patency with high level laryngeal neuromuscular stimulation. (inf – sup = inferior to superior, ms = millisecond, PCA = posterior cricoarytenoid, post – ant = posterior to anterior, TA = thyroarytenoid).
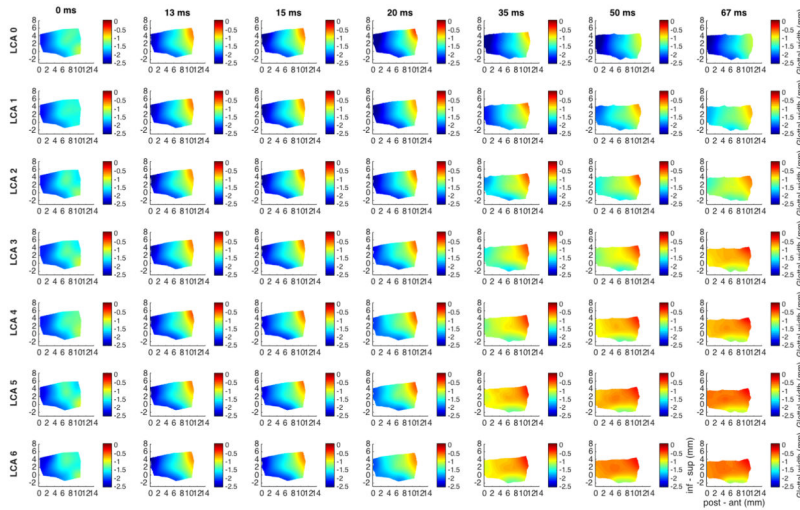
Fig. 7.
Glottal shape for the interaction between maximal CT activation and graded LCA activation. Design layout is same as Fig.1 except now CT is held at maximum stimulation for all rows (grade 6), while LCA is added in a graded fashion from grade 0 ('LCA 0', row 1) to grade 6 ('LCA 6', row 7). Duration of recording is 67 ms in order to capture full spectrum of posture changes. CT alone (row 1) results in 16% abduction, 12% lengthening, and 4-13% thinning of the vocal fold. LCA activation adducts the mid vocal fold to 63%. Increased LCA activation also augments vocal fold thinning throughout the anteroposterior glottal axis to as much as 18%. Adductory effect of LCA with full CT activation yields overall a more homogenous adduction in the anteroposterior glottal axis as opposed to its usual more posterosuperiorly based adduction with LCA acting alone. (CT = cricothyroid, inf – sup = inferior to superior, LCA = lateral cricoarytenoid, ms = millisecond, post – ant = posterior to anterior).
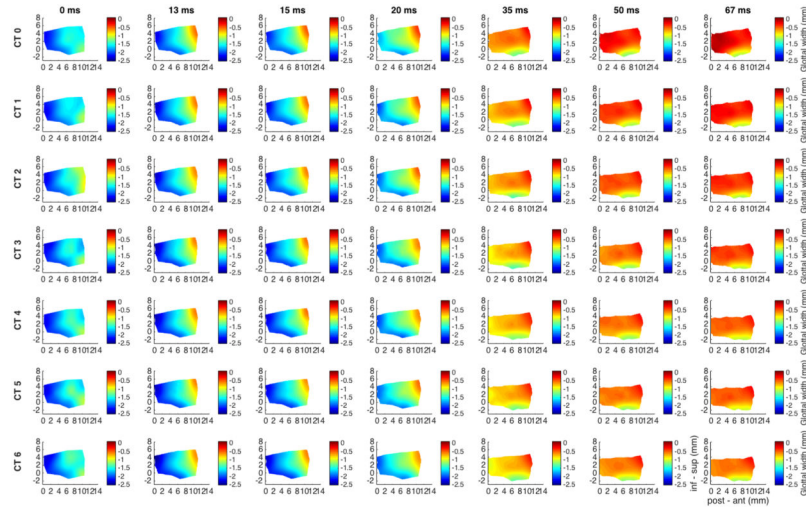
Fig. 8.
Glottal shape for the interaction between maximal LCA activation and graded CT activation. Design layout is same as Fig.1 except now LCA is held at maximum stimulation for all rows (grade 6), while CT is added in a graded fashion from grade 0 ('CT 0', row 1) to grade 6 ('CT 6', row 7). The LCA itself does not change the length of the vocal fold, however with increasing CT activation the vocal fold is lengthened up to 7%. LCA alone (row 1) causes 88% adduction which is reduced by 25% (to 63%) with full grade 6 CT activation. LCA results in vertical thickness thinning by 5-7%. This thinning is further augmented by CT activation to 19%. Again, CT activation helps distribute the posterosuperior effect of LCA more evenly along the glottal axis. (CT = cricothyroid, inf – sup = inferior to superior, LCA = lateral cricoarytenoid, ms = millisecond, post – ant = posterior to anterior).